Thermonuclear ignition and the onset of propagating burn in inertial fusion implosions

A. R. Christopherson, R. Betti, and J. D. Lindl

Phys. Rev. E **99**, 021201 — Published 25 February 2019

DOI: 10.1103/PhysRevE.99.021201

Thermonuclear ignition and the onset of propagating burn in inertial fusion implosions

A. R. Christopherson[1,3],R. Betti[1,2,3], J. D. Lindl[4]
[1]*Dept. Mechanical Engineering, University of Rochester, Rochester NY 14627*
[2]*Dept. Physics and Astronomy, University of Rochester, Rochester NY 14627*
[3]*Laboratory for Laser Energetics, University of Rochester, Rochester NY 14623*
[4]*Lawrence Livermore National Laboratory, Livermore, California 94550, USA*

Separating ignition of the central hot spot from propagating burn in the surrounding dense fuel is crucial to conclusively assess the achievement of ignition in inertial confinement fusion (ICF). We show that the transition from hot spot ignition to the onset of propagating burn occurs when the alpha heating within the hot spot has amplified the fusion yield by 15 to 25x with respect to the compression-only case without alpha energy deposition. This yield amplification corresponds to a value of the fractional alpha energy $f_\alpha \approx 1.4$ ($f_\alpha = 0.5$ alpha energy/hot spot energy). The parameter f_α can be inferred in ICF experiments by measuring the neutron yield, hot spot size, temperature, and burn width. This ignition threshold is measurable and applicable to all ICF implosions of DT-layered targets both direct and indirect drive. The results of this paper can be used to set the goals of the ICF effort with respect to the first demonstration of thermonuclear ignition.

PACS numbers:

A large effort is currently under way to demonstrate thermonuclear ignition in the laboratory via inertial confinement fusion (ICF) [1]. ICF uses laser-driven implosions of a solid deuterium-tritium (DT) shell to achieve ignition conditions [2, 3]. Ignition is a thermal instability of a DT plasma driven by the energy deposition of the alpha particles ("alpha heating") produced by the fusion reaction D+T=α(3.5MeV)+n(14.1MeV). Ignition has never been achieved in a laboratory plasma and its demonstration is widely viewed as a major scientific achievement with important applications to fusion energy generation and to the stewardship of the nuclear stockpile. Unlike in steady state plasmas, as those envisioned for magnetic confinement fusion [4], assessing ignition in ICF is greatly complicated by the transient nature of implosions and the fact that ignition starts from the central hot region ("hot spot ignition") and then propagates to the cold and dense surrounding fuel ("burn wave propagation"). The fundamental mechanism at the basis of ignition is alpha heating of the DT fuel and its positive feedback on the fusion reaction rate.

Current experiments at the National Ignition Facility (NIF) have demonstrated significant alpha heating leading to amplifications of the fusion yield close to 3 folds [5–7]. Despite much work on assessing and measuring the degree of alpha heating, there are two crucial questions still unanswered with regard to ignition: (1) what is ignition in inertial fusion and (2) what fusion yields are required in ICF to claim that ignition has taken place. Existing metrics such as the generalized Lawson criterion χ [8–10] or the Ignition Threshold Factor ITFx [11] are often incorrectly referred to as "ignition metrics." They were developed to assess the underlying hydrodynamics required for high yields and they are used as design tools. Both χ and $ITFx$ were evaluated from simulations with alpha energy deposition off (no-alpha metrics) and correlated to the fusion yields from simulations with alpha deposition on [9, 12]. They are not measureable criteria since ignition experiments are affected by alpha heating and they are not ignition metrics because they only identify generic yield enhancements from alpha heating. In Refs [12–14], these metrics were converted into measureable forms but their use was and still is limited to evaluating the degree of alpha heating through the yield amplification $\hat{Y}_{amp} \equiv Y_\alpha / Y_{no\alpha}$ caused by alpha heating. Here Y_α is the fusion yield measured in an experiment and $Y_{no\alpha}$ is the estimated yield without accounting for alpha particle energy deposition. The $no\alpha$ yield cannot be measured but it is estimated through numerical simulations where the alpha deposition is turned off. Although both $ITFx$ and χ were shown to be correlated with the yield amplification in the presence of alpha heating, they could not identify the alpha heating levels required for ignition when applied to a given target.

Other engineering definitions of ignition, such as Target Gain=1, have also been often used in the past [15]. Here, target gain is the ratio of the fusion energy output to the laser energy on target. Such a metric is not rooted in the burning-plasma physics of DT fuel and is unrelated to the onset of ignition. It is only motivated by its implications to fusion energy, where an energy output greater than the input is required for any viable fusion scheme. This metric is not an indicator of the onset of the thermonuclear instability and therefore it cannot be used to measure the ignition point. As currently described, existing metrics are not valid ignition metrics since they do not identify the ignition point. It follows that a clear physical and measureable definition of ICF ignition needs to be identified.

In this Letter, we try to answer both questions. We first provide a physical definition of hot spot ignition in ICF and then develop a metric to identify the ignition point. We also provide an approximate formula for the fusion energy yield corresponding to the ignition point.

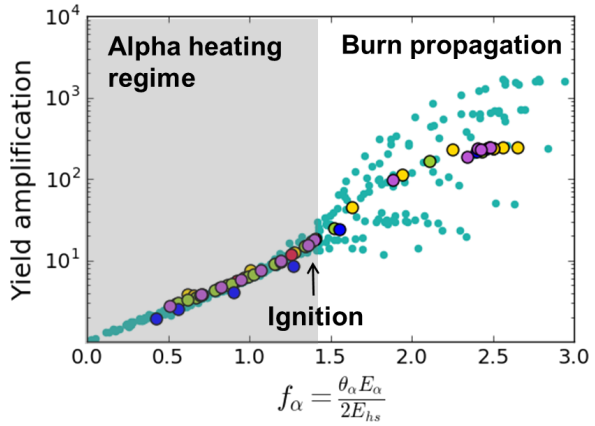

FIG. 1: The yield amplification is plotted as a function of f_α for the ensemble of 1-D LILAC [18] simulations (turquoise points). In the alpha-heating regime ($f_\alpha < 1.4$), the yield amplification depends uniquely on f_α regardless of the target mass, areal density, and temperature. After $f_\alpha = 1.4$, shell mass and burnup fraction determine the maximum fusion yield. The yellow, red, green, and dark blue points respectively represent 2-D DRACO [19] single mode simulations of modes 2, 4, 6, and 10. The purple points are multi-mode simulations perturbed by modes 2 and 4.

The definition of ignition is of general validity for laser fusion and it identifies the onset of the thermal runaway within the hot spot of an ICF implosion just prior to the burn propagation in the dense fuel. It is shown in this Letter that the onset of burn propagation can be uniquely identified through the dimensionless parameter

$$f_\alpha \equiv \frac{1}{2}\frac{\theta_\alpha E_\alpha}{E_{hs}}, \tag{1}$$

where E_α is the total alpha-particle energy, θ_α is the fraction of alpha particles deposited into the hot spot, and E_{hs} is the hot spot internal energy at bang time (when the neutron production rate is maximized). Ignition occurs at the critical value $f_\alpha \approx 1.4$ corresponding to a yield amplification due to alpha heating of about 15x to 25x. For $f_\alpha < 1.4$, alpha-heating is mostly confined to the hot spot while for $f_\alpha > 1.4$, ablation of shell mass into the neutron producing region increases the fusion output significantly. The parameter f_α can be inferred from experimental observables and it can be used to identify ignition of the hot spot in all ICF implosions of DT-layered targets. We also derive a formula relating the fusion yields of marginally ignited targets to their areal density and fuel mass.

To identify the ignition point, we first search for qualitative features distinguishing runaway burn in the entire fuel volume from sub-ignition alpha heating. The first distinctive feature is related to the different behavior of the yield amplification for implosions in the alpha heating regime versus implosions with propagating burn. It was shown in Ref [13] that in the alpha heating regime, the yield amplification depends uniquely on the dimensionless parameter f_α. In the runaway burn phase, rapid ablation of shell material into the hot spot qualitatively changes the fuel assembly into a system where the hot spot density is comparable to the shell density. The final burnup fraction Φ = neutron yield/N_{DT}^{tot} is then determined by considering the amount of fusion reactions that occur in a compressed plasma before it disassembles. This calculation is described in Ref. [2] and gives

$$\Phi \simeq \frac{\rho R}{\rho R + H_B}, \tag{2}$$

where ρR is the total fuel areal density, $H_B \sim \sqrt{T}/\langle\sigma v\rangle$ is the burn parameter, T is the plasma temperature, and $\langle\sigma v\rangle$ is the fusion reactivity [16] (typically H_B is taken to be 6 or 7). In this case, the burn-up fraction becomes the dominant factor in determining the yield amplification. Therefore, given the unique role that f_α plays in describing the alpha heating regime, it is expected that this would no longer be the case after ignition and subsequent burn propagation. This leads to the observation that the yield amplification versus f_α curves for different implosions overlap during the alpha heating phase up to ignition and then separate during the burn propagation. This is verified in Fig. 1 where the yield amplification curves for many different targets are shown to overlap up to a critical value of $f_\alpha \simeq 1.4$. The 1-D simulation ensemble shown here contains implosion velocities between 200 km/s and 600 km/s, laser energies between 30 kJ and 10 MJ, and adiabats between 1 and 6 where the adiabat is given for DT by $\alpha = P/2.2\rho^{5/3}$, with the shell pressure P in megabars and the plasma density in g/cm^3 [17]. The 1-D database was generated by creating many ignited implosions with a variety of different target gains and then degrading them by reducing the implosion velocity or increasing the adiabat. The red, purple, green, dark blue, and yellow points are 2-D simulations of ignited targets degraded by single modes applied to the inner shell surface.

The parameter f_α is designed to compare the deposited alpha energy to the hot spot internal energy at bang time. In the numerator, $E_\alpha = \varepsilon_\alpha Yield$ where $\varepsilon_\alpha = 3.5$ MeV and $Yield$ is the neutron yield. The factor 1/2 accounts for the fact that approximately one half of all of the fusion alphas produced have deposited their energy into the hot spot at bang time. In defining E_{hs}, the hot spot radius is the point where the neutron production rate drops to 17% of its maximum value. The lagrangian trajectory of this hot spot is then back calculated in time to determine the fraction of alpha particles absorbed in the hot spot, as was done in Ref. [20]. The fraction of alpha particles absorbed into the hot spot is calculated as

$$\theta_\alpha \equiv \frac{\int_0^{t_{bang}} W_{\alpha,hs}(t)dt}{\int_0^{t_{bang}} W_{\alpha,tot}(t)dt}, \tag{3}$$

where t_{bang} is the bang time when the neutron production rate is maximized, $W_{\alpha,hs}(t)$ is the alpha deposition rate into the lagrangian hot spot mass at time t, and $W_{\alpha,tot}(t)$

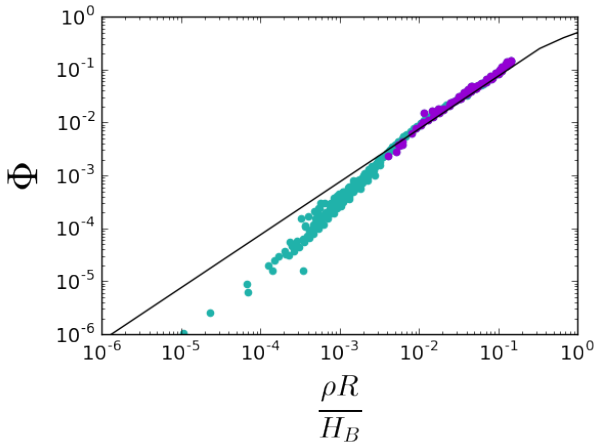

FIG. 2: In the burn propagation phase, the fuel burnup fraction Φ depends uniquely on the parameter $\rho R/H_B$ and follows the same scaling as predicted by theory (Eq. (2)). Here, the burnup fraction is defined as $\Phi = Yield/N_{DT}$, where N_{DT} is the initial number of DT ions in the unablated mass. The dark violet points correspond to implosions with yield amplifications larger than 25 and the black line is the analytic curve from Eq. (2).

is the total alpha deposition rate in the entire simulation domain at time t. This is an exact calculation of the alpha energy deposited into the hot spot mass in the presence of ablation of shell material into the hot spot.

In 1D, the majority of alpha particles are absorbed by the hot spot since the alphas leaking from the hot spot deposit their energy into a thin inner shell layer that is subsequently ablated into the hot spot. For a hot spot radius defined by the neutron R17 contour, typical values of θ_α range from 0.8 to 1. For distorted implosions, the fraction of absorbed alphas can vary significantly and needs to be evaluated. For simplicity here, we do not consider implosions with yield-over-clean (YOC) less than 50 % because there are no expectations that such highly distorted implosions can approach ignition conditions on NIF. Here, the YOC = *perturbed yield/ 1D clean yield* is calculated without accounting for alpha energy deposition to better measure the level of nonuniformities independently of the proximity to ignition.

The next step is to investigate the nature of these qualitative changes occurring at $f_\alpha = 1.4$ and $\hat{Y}_{amp} = 15$ to 25. The dependence of the fusion yield on areal density and temperature is illustrated in Fig. 2 where the fuel burnup fraction Φ is plotted against the parameter $\rho R/H_B$ and compared with Eq. (2). Implosions in the alpha heating phase (where the burnup fraction is low) deviate from Eq. (2), while in the burn propagation phase (with yield amplifications > 25), a close relationship is observed between the fuel burnup Φ and the parameter $\rho R/H_B$ following Eq. (2). This supports the conclusion that after burn propagation occurs, the fusion yield is determined by Eq. (2) instead of the ignition parameter f_α.

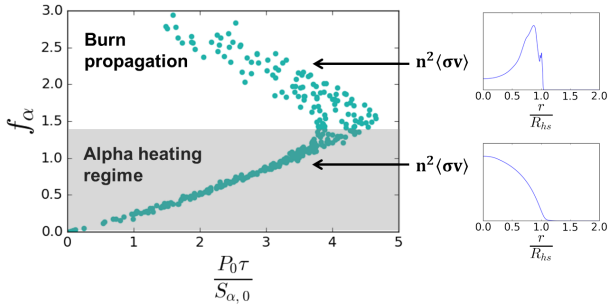

FIG. 3: The metric f_α is plotted against the intrinsic parameter $P_0\tau/S_{\alpha,0}$. At $f_\alpha \sim 1.4$, this profile factor changes dramatically and the tight correlation observed between f_α and $P_0\tau/S_{\alpha,0}$ breaks down. Toward the right, example profiles of the neutron production rate per unit volume are shown to illustrate that the neutron production rate is maximized near the hot spot edge.

Another way to interpret the transition at $f_\alpha \sim 1.4$ is to examine how f_α compares to $P_0\tau/2S_{\alpha,0}$ evaluated at the center of the hot spot where $S_{\alpha,0} = 24T_0^2/\varepsilon_\alpha \langle\sigma v\rangle_0$. Here, P_0, T_0, and $\langle\sigma v\rangle_0$ denote the central hot spot pressure, temperature, and fusion reactivity evaluated at bang time and τ is the FWHM of the neutron production rate. Note that $P_0\tau/2S_{\alpha,0}$ is related to f_α via the following relation:

$$f_\alpha = \frac{1}{2}\frac{P_0\tau}{S_{\alpha,0}}\mu_\alpha, \tag{4}$$

where μ_α depends only on spatial profiles and it is given by

$$\mu_\alpha \equiv \frac{T_0^2}{P_0^2\langle\sigma v\rangle_0 V_{hs}}\int P^2\frac{\langle\sigma v\rangle}{T^2}dV_{hs}. \tag{5}$$

Here, the ideal gas equation of state is used in the hot spot $P = 2nT$ with n representing the ion number density for a 50-50 DT plasma. The fusion production rate $n^2\langle\sigma v\rangle$ is proportional to $P^2\langle\sigma v\rangle/T^2$ and is spatially dependent on the temperature for a flat pressure (isobaric) profile.

Figure 3 shows a tight correlation between f_α and $P_0\tau/2S_{\alpha,0}$ up to the ignition point where $f_\alpha \sim 1.4$ and a distinct maximum in $P_0\tau/2S_{\alpha,0}$ occurs. At the ignition point, the central hot spot temperature corresponding to the maximum value of $P_0\tau/2S_{\alpha,0}$ in Fig. 3 varies between 10 and 17 keV in our database. This is not surprising, considering that S_α is minimized around 14 keV. Therefore, as a result of the runaway amplification in temperature, an important feature of the onset of burn propagation is that the central temperature reaches the value of ~ 14 keV, corresponding to the minimum value of $S_{\alpha,0}$. Consequently, the peak of the fusion reaction rate shifts towards the denser regions (i.e. the shell). This is also illustrated in the inserts of Fig. 3 where it is shown that the burn profile is peaked in the center in the alpha heating phase and peaked at the hot spot

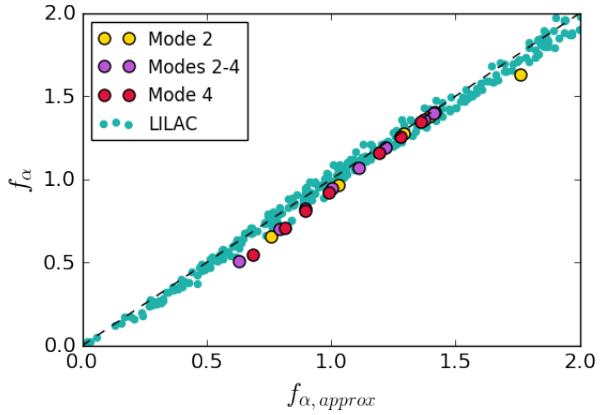

FIG. 4: The metric f_α computed using the pressure from Eq. (6) compares well with exact calculations from LILAC (turquoise dots) as well as 2D single mode and multi-mode simulations.

edge during the burn propagation phase. This indicates that alpha heating, with respect to power losses, is more dominant in the shell than it is in the low density hot spot.

To experimentally assess the achievement of ignition, the parameter f_α needs to be inferred from experimental observables. The total alpha energy is $E_\alpha = \varepsilon_\alpha \cdot Yield$ and the pressure can be inferred from the neutron yield, ion temperature T_i, hot spot volume V_{hs}, and burn duration (or confinement time) τ as described in Ref. [21]:

$$\langle P\rangle_{approx} \approx \sqrt{\frac{16\cdot Yield\cdot T_i^2}{\tau V_{hs}\langle\sigma v\rangle}}. \qquad (6)$$

In Figure 4, the exact value of f_α from 1D and 2D simulations is plotted against the approximate formula from experimental observables. Here, $f_{\alpha,approx}$ is defined as

$$f_{\alpha,approx} \equiv \theta\frac{0.5E_\alpha}{1.5\langle p\rangle_{approx}V_{hs}} \approx \frac{0.31E_\alpha}{\langle p\rangle_{approx}V_{hs}}, \qquad (7)$$

where $\theta = 0.93$ gives the best least squares fit for $f_\alpha \le 1.4$. Fig. 4 shows that $f_{\alpha,approx}$ approximates the exact f_α well in both 1-D and distorted 2-D simulations. Eq. (7) is applicable to implosions with modest levels of low-mode asymmetries (YOC>0.5). Highly distorted implosions require a more detailed analysis for inferred θ_α that will be discussed in a separate paper. It should also be noted that modifications to the definition of pressure will correspond to different values of f_α required for ignition [22].

The next step is to determine the fusion output required to achieve ignition. We start from the simple consideration that near the ignition point, rather small changes to the implosion hydrodynamic performance result into significant variations in the alpha heating levels and fusion yields. This occurs because of the thermal runaway triggered by the ignition process when the alpha energy is deposited. Therefore, if we consider $no\alpha$ properties, such as the "theoretical" fusion yield in the absence of alpha deposition $Y_{no\alpha}$, their magnitude does not vary significantly as the ignition point is crossed. One can think of $no\alpha$ properties [10] as slowly varying with respect to the fast varying $with-\alpha$ properties. It follows that the ignition conditions in terms of $no\alpha$ properties occurs in the neighborhood of $\chi_{no\alpha} \sim 1$ where $\chi_{no\alpha}$ is derived from the Lawson criterion in Refs [8, 20, 23] and can be written as

$$\chi_{no\alpha} = (\rho R)^{0.61}\left(\frac{0.12Yield_{16}}{M_{stag}}\right)^{0.34}, \qquad (8)$$

where M_{stag} is the stagnated DT mass in mg, ρR is the neutron averaged fuel areal density in g/cm^2, and $Yield_{16}$ is the neutron yield in units of 10^{16} neutrons. All quantities are evaluated without accounting for alpha heating. Equation (8) can be used to infer the $no\alpha$ yield near ignition by setting $\chi_{no\alpha} \approx 1$. Since, as shown earlier, the yield amplification corresponding to the ignition point $f_\alpha = 1.4$ is about 20, we can determine the fusion energy yield required for ignition as $Y_{ign} \approx 20M_{stag}\chi^3_{no\alpha}/(0.12(\rho R)^{1.8})$. To account for the variations in $\chi^3_{no\alpha}$ near the ignition point, we adjust the coefficients to fit the simulation results. Accurate to approximately 15%, this leads to the following formula for the fusion yield required for ignition:

$$Y_{ign}(MJ) \approx \left(\frac{M_{stag}(mg)}{0.21}\right)^{0.81}\left(\frac{1}{\rho R(g/cm^2)}\right)^{2.61}. \qquad (9)$$

Since the areal density and stagnating mass do not include the effect of alpha heating, Eq. (9) can be used to estimate the fusion yield required for ignition in current indirect drive NIF implosions whose areal density is little affected by alpha heating. In such implosions, the areal density varies from 0.5 g/cm^2 to 1.3 g/cm^2. The required fusion yield output needed for ignition is tabulated in Table 1 for several different values of areal density and stagnated mass characteristic of current ICF campaigns on the NIF [5, 6, 24, 25]. Note that the fusion

TABLE I: Fusion yields required for ignition for targets typical of current ignition experiments on the NIF

DT mass	Shell areal density	Required fusion yield
0.1 mg	0.6 g/cm^2	2.1 MJ
0.1 mg	0.9 g/cm^2	0.7 MJ
0.1 mg	1.2 g/cm^2	0.3 MJ
0.2 mg	0.6 g/cm^2	3.6 MJ
0.2 mg	0.9 g/cm^2	1.3 MJ
0.2 mg	1.2 g/cm^2	0.6 MJ

yield required for ignition increases sharply at lower areal densities. While low-convergence low-ρR implosions are more predictable and have demonstrated higher yields through higher implosion velocities, their poor confinement and low convergence sharply increase the fusion yield requirements for ignition.

In summary, the ignition condition for inertially confined plasmas has been identified as the transition from thermal instability of the hot spot to propagating burn in the shell. Using 1-D and 2-D radiation hydrodynamic simulations, it was shown that the onset of ignition can be assessed using measureable parameters through the quantity $f_\alpha = 1/2\theta_\alpha E_\alpha/E_{hs}$. Ignition corresponds to a yield amplification of 15x to 25x and a value of $f_\alpha \simeq 1.4$.

This work was supported by the U.S. Department of Energy under Contract No. DE-SC0016258,under Cooperative Agreement No. DE-NA0001944, the University of Rochester, and the New York State Energy Research and Development Authority. This support does not constitute an express or implied endorsement on the part of DOE.

[1] J.H. Nuckolls, L. Wood, A. Thiessen, G.B. Zimmermann, Nature **239**, 139(1972)
[2] S. Atzeni and J. Meyer-ter-vehn, *The Physics of Inertial Fusion* (Clarendon, Oxford, 2004); J. D. Lindl, *Inertial Confinement Fusion* (Springer, New York, 1998)
[3] J.D. Lawson, *Proc. Phys. Soc. London* B **70**, 6 (1957)
[4] J. Ongena, R. Koch, R. Wolf, and H. Zohm, Nature Physics, **12**, 398-410 (2016).
[5] S. Le Pape, L. F. Berzak-Hopkins, L. Divol, A. Pak, E. L. Dewaald, S. Bhandarkar, L. R. Bennedetti, T. Bunn, J. Biener, J. Crippen, et al, Phys. Rev. Lett. **120**, 245003 (2018).
[6] T. Doppner, D. A. Callahan, O. A. Hurricane, D. E. Hinkel, T. Ma, H. S. Hark, L. F. Berzak-Hopkins, D. T. Casey, P. Celliers, E. L. Dewald, et al, Phys Rev Let, **115**, 055001 (2015).
[7] O. A. Hurricane, D. A. Callahan, D. T. Casey, P. M. Celliers, C. Cerjan, E. L. Dewald, T. R. Dittrich, T. Doppner, D. E. Hinkel, L. F. B. Hopkins et al, Nature **506**, 343 (2014)
[8] C. Zhou, R. Betti, Phys. Plasmas **15**, 102707 (2008)
[9] P. Y. Chang, R. Betti, B. K. Spears, K. S. Anderson, J. Edwards, M. Fatenejad, J. D. Lindl, R. L. McCrory, R. Nora, and D. Shvarts, Phys. Rev. Lett. **104**, 135002 (2010)
[10] R. Betti, P. Y. Chang, B. K. Spears, K. S. Anderson, J. Edwards, M. Fatenejad, J. D. Lindl, R. L. McCrory, R. Nora, and D. Shvarts, Phys. Plasmas **17**, 058102 (2010)
[11] B. K. Spears, S. Glenzer, M. J. Edwards, S. Brandon, D. Clark, R. Town, C. Cerjan, R. Dylla-Spears, E. Mapoles, D. Munro et al., Phys. Plasmas **19**, 056316 (2012)
[12] J.D. Lindl, O. Landen, J. Edwards, E. Moses and the NIC Team, Phys. Plasmas 21, 020501 (2014) and Phys. Plasmas 21, 129902(E) (2014)
[13] A. R. Christopherson, R. Betti, J. Howard, K. M. Woo, A. Bose, E. M. Campbell, and V. Gopalaswamy, Phys. Plasmas **25**, 072704 (2018).
[14] R. Betti, A. R. Christopherson, B. K. Spears, R. Nora, A. Bose, J. Howard, K. M. Woo, M. J. Edwards, and J. Sanz, Phys. Rev. Lett., **114**, 25503 (2015).
[15] "An assessment of the prospects for Inertial Fusion Energy", National Research Council, The National Academies Press, Washington DC (2013).
[16] H. S. Bosch and G. M. Hale, Nucl Fusion **32** 611 (1992).
[17] M. C. Hermann, M. Tabak, and J. D. Lindl, Nucl. Fusion **41**, 99 (2001).
[18] J. Delettrez, R. Epstein, M. C. Richardson, P. A. Jaanimagi, and B. L. Henke, Phys. Rev. A **36**, 3926 (1987)
[19] P.B. Radha, T.J.B. Collins, J.A. Delettrez, Y. Elbaz, R. Epstein, V.Yu. Glebov, V.N. Goncharov, R.L. Keck, J.P. Knauer, and J.A. Marozas et al., Phys. Plasmas **12**, 056307 (2005).
[20] A. R. Christopherson, R. Betti, A. Bose, J. Howard, K. M. Woo, E. M. Campbell, J. Sanz, and B. K. Spears, Phys. Plasmas. **25**, 012703 (2018).
[21] C. Cerjan, P. T. Springer, and S. M. Sepke, Phys. Plasmas **20**, 056319 (2013)
[22] J. D. Lindl, S. Haan, O. Landen, A. R. Christopherson, and R. Betti, accepted for publication in Phys. Plasmas
[23] R. Betti, Theory of ignition and hydro-equivalence for inertial confinement fusion, paper presented at the 24th IAEA Fusion Energy Conference, San Diego, CA, 813 October 2012.
[24] M. J. Edwards, P. K. Patel, J. D. Lindl, L. J. Atherton, S. H. Glenzer, S. W. Haan, J. D. Kilkenny, O. L. Landen, E. I. Moses, A. Nikroo, et al, Phys. Plasmas **20**, 070501 (2013).
[25] K. L. Baker, C. A. Thomas, D. T. Casey, S. Khan, B. K. Spears, R. Nora, T. Woods, J. L. Milovich, R. L. Berger, D. Strozzi, D. Clark, et al, Phys. Rev. Lett, **121**, 135001 (2018).